

JPET #153973

Title Page:

**The Binding Specificity and Selective Antagonism of Vedolizumab, an Anti- $\alpha_4\beta_7$ Integrin
Therapeutic Antibody in Development for Inflammatory Bowel Diseases**

Dulce Soler, Tobias Chapman, Li-Li Yang, Tim Wyant, Robert Egan and Eric R. Fedyk.

Millennium Pharmaceuticals Inc., A Takeda Pharmaceuticals Company, 40 Landsdowne St.
Cambridge, MA 02139

JPET #153973

a) Running Title Page

Binding and Inhibitory Properties of Vedolizumab

b) Corresponding author

Eric R. Fedyk, Ph.D.

Millennium Pharmaceuticals Inc.

40 Landsdowne Street

Cambridge, MA 02139

USA

Tel: 617-551-8685

Fax: 617-444-1501

E-mail: fedyk@mpi.com

c) Manuscript extent

Text pages – 41

Tables – 1

Figures – 8

References – 40/40

Words in the abstract – 249/250

Words in the introduction – 747/750

Words in the discussion – 1,291/1,500

JPET #153973

d) Nonstandard abbreviations used

BSA – Bovine serum albumin

CD – Crohn's disease

CDR – Complementary determining region

DMEM – Dulbecco's modified eagle medium

Fc – Fragment crystallizable

GI – Gastrointestinal

GMFI – Geometric mean fluorescence intensity

IBD – Inflammatory bowel disease

IC₅₀ – Median inhibition concentration

mAb – monoclonal antibody

MAdCAM-1 – Mucosal vascular addressin cell adhesion molecule 1

PBMC – Peripheral blood mononuclear cell

PBS – Phosphate buffered saline

PMA – phorbol 12-myristate 13-acetate

Th17 – T-helper 17

UC – Ulcerative colitis

VCAM-1 – Vascular cell adhesion molecule 1

e) Recommended section assignment

Gastrointestinal, Hepatic, Pulmonary, and Renal

JPET #153973

Abstract

Vedolizumab is a humanized monoclonal antibody that targets the $\alpha_4\beta_7$ integrin exclusively, and modulates inflammation in the gastrointestinal tract without inducing the systemic immunosuppression that characterizes anti- α_4 chain monoclonal antibodies, such as natalizumab. This unique pharmacologic profile is largely attributable to four determinants. Expression of the $\alpha_4\beta_7$ integrin is restricted to subsets of leukocytes. Vedolizumab did not bind to the majority of memory $CD4^+$ T lymphocytes (60%), neutrophils and most monocytes. The highest level of vedolizumab binding was to a subset (~25%) of human peripheral-blood memory $CD4^+$ T lymphocytes that included gut-homing interleukin 17 T helper lymphocytes. Vedolizumab also bound to eosinophils at high levels, and to naïve helper T lymphocytes, naïve and memory cytotoxic T lymphocytes, B lymphocytes, natural killer cells, and basophils at lower levels; vedolizumab bound to memory $CD4^+$ T and B lymphocytes with subnanomolar potency (EC_{50} = 0.3 to 0.4 nM). The second determinant is binding specificity; vedolizumab binds exclusively to the $\alpha_4\beta_7$ integrin, and not to the $\alpha_4\beta_1$ and $\alpha_E\beta_7$ integrins. The third determinant is selective antagonism; vedolizumab selectively inhibited adhesion of $\alpha_4\beta_7$ -expressing cells to mucosal addressin cell adhesion molecule 1 (MAdCAM-1) (median inhibition concentration [IC_{50}] = 0.02 to 0.06 μ g/ml) and fibronectin (IC_{50} = 0.02 μ g/ml), but not vascular cell adhesion molecule 1 (VCAM-1). The fourth determinant is the gastrointestinal-specific tropism of the $\alpha_4\beta_7$ integrin function. These pharmacologic properties of vedolizumab, in conjunction with the gastrointestinal-tropism of $\alpha_4\beta_7$ integrin function, may ultimately confer an improved risk-to-benefit profile for patients with inflammatory bowel diseases.

JPET #153973

Introduction

The inflammatory bowel diseases (IBDs), ulcerative colitis (UC) and Crohn's disease (CD), are chronic diseases of the gastrointestinal (GI) tract characterized by an exacerbated inflammatory cell infiltrate in the gut mucosal tissue (Xavier and Podolsky, 2007). Multiple inflammatory cell types, including neutrophils, macrophages, dendritic cells, and lymphocytes, participate in the pathogenesis of IBD, with lymphocytes having a central role in the induction and maintenance of the chronic inflammatory process in the lamina propria (Xavier and Podolsky, 2007). Infiltration of the GI tract by T lymphocytes is a well-documented pathogenic mechanism of IBD, and the molecular mechanisms by which these lymphocytes enter the gut are distinct from those in other peripheral tissues, such as the skin and central nervous system (Butcher and Picker, 1996; Engelhardt et al., 1998; Engelhardt and Briskin, 2005; Salmi and Jalkanen, 2005; Agace, 2006). The complex infiltration process in the GI tract requires the coordinated interaction of several adhesion and signaling molecules on the surface of T lymphocytes (selectins, integrins, chemokine receptors) with their corresponding ligands on the endothelium. The $\alpha_4\beta_7$ integrin mediates the infiltration of the GI tract by memory T lymphocytes, by binding to mucosal addressin cell adhesion molecule 1 (MAdCAM-1) on endothelial cells, and blockade of this interaction provides efficacy in animal models of IBD (Hesterberg et al., 1996; Picarella et al., 1997), and in patients with UC (Feagan et al., 2005) and CD (Feagan et al., 2008).

The $\alpha_4\beta_7$ integrin is consequently an ideal therapeutic target for IBD and is currently being targeted through three different strategies. Two of these strategies target either the α_4 chain or the β_7 chain. They are not specific for the $\alpha_4\beta_7$ integrin and bind to other integrins containing

JPET #153973

these chains, specifically the $\alpha_4\beta_1$ and $\alpha_E\beta_7$ integrins. The $\alpha_4\beta_1$ and $\alpha_E\beta_7$ integrins mediate effects within and outside the GI tract. The $\alpha_E\beta_7$ integrin is postulated to locate and retain T lymphocytes within the epithelium of numerous tissues, by binding E-cadherin on the basolateral surface of epithelial cells (Kilshaw, 1999). The $\alpha_4\beta_1$ integrin mediates extravasation of lymphocytes, monocytes, and eosinophils into numerous types of tissues by binding to vascular cell adhesion molecule 1 (VCAM-1) expressed on the luminal surface of endothelium, and to fibronectin within extracellular matrix (Gonzalez-Amaro et al., 2005). Antagonizing the $\alpha_4\beta_1$ or $\alpha_E\beta_7$ integrin thus has a systemic effect.

The humanized anti- α_4 antibody, natalizumab, elicits effects in numerous tissues, including leukocytosis (Ghosh et al., 2003; Sandborn et al., 2005; Targan et al., 2007), mobilization of hematopoietic stem cells (Bonig et al., 2008; Zohren et al., 2008), and inhibition of leukocyte trafficking into the central nervous system (del Pilar Martin et al., 2008). Indeed, antagonizing both the $\alpha_4\beta_1$ and $\alpha_4\beta_7$ integrins may explain efficacy in the central nervous system (Miller et al., 2003) and the GI tract, respectively (Ghosh et al., 2003; Sandborn et al., 2005; Targan et al., 2007). However, administration of natalizumab is associated with systemic immunosuppression; for example, increased incidence of the fatal infectious disease progressive multifocal leucoencephalopathy (PML) (Berger and Korolnik, 2005; Kleinschmidt-DeMasters and Tyler, 2005; Langer-Gould et al., 2005; Ransohoff, 2005; Van Assche et al., 2005). It is postulated that the anti-inflammatory mechanism driving the efficacy of natalizumab in multiple sclerosis may also predispose patients to progressive multifocal leucoencephalopathy by decreasing immunosurveillance in the central nervous system (Berger, 2006; Berger and Houff, 2006; Korolnik, 2006; Niino et al., 2006; Stuve et al., 2006a; Stuve et al., 2006b; del Pilar Martin et al., 2008).

JPET #153973

A third strategy is exclusive targeting of the $\alpha_4\beta_7$ integrin, which is utilized by vedolizumab (former versions known as MLN0002, MLN02, and LDP-02). Vedolizumab is a humanized version of Act-1, a mouse antibody (Lazarovits et al., 1984) that binds to a conformational epitope that is unique to the heterodimerization of the human α_4 chain with the β_7 chain (Schweighoffer et al., 1993; Tidswell et al., 1997). Act-1 therefore binds specifically to the $\alpha_4\beta_7$ integrin, and administration to colitic cotton-top tamarins leads to the resolution of disease (Hesterberg et al., 1996). Vedolizumab binds to the $\alpha_4\beta_7$ integrin on peripheral-blood lymphocytes and inhibits adhesion of the lymphocyte to MAdCAM-1. Humanized Act-1 has demonstrated statistically significant efficacy in placebo-controlled phase 2 clinical trials of patients with moderately active UC (Feagan et al., 2005) and in patients with moderately active CD (Feagan et al., 2008). The enhanced specificity of vedolizumab may ultimately confer an improved risk-to-benefit ratio for patients with IBD. The data reported herein characterize the binding specificity and potency of vedolizumab and the associated selective antagonism of adhesion.

JPET #153973

Methods

Proteins and Antibodies. Ninety-six-well plates coated with recombinant human VCAM-1/fragment crystallizable (Fc) chimera protein, an alternatively-spliced form of human fibronectin containing the CS-1 peptide, and unlabeled blocking antibodies to human VCAM-1, α_4 and β_1 were obtained from R&D Systems (Minneapolis, MN). A MAdCAM-1/mFc fusion protein was available in-house. Fluorochrome-conjugated anti-mouse IgG was purchased from Jackson ImmunoResearch (West Grove, PA). Pharmlyse buffer was obtained from BD Biosciences (San Jose, CA). Fluorochrome-conjugated antibodies to human proteins were purchased from various sources: mouse antibodies to CD4 (L200), CD8 (SK1), CD14 (M ϕ P9), CD19 (HIB19), CD45R0 (UCHL1), CD49d (α_4 ; L25), CD56 (NCAM16.2), and CD103 (α_E ; Ber-ACT8) and a rat antibody to β_7 (FIB504) from BD Biosciences (San Jose, CA); mouse antibody to CD29 (β_1 ; MEM-101A) from eBioscience (San Diego, CA); mouse antibody to CD123 (AC145) from Miltenyi Biotech (Auburn, CA); mouse antibodies to CD49d (α_4 ; 2B4), CD29 (β_1 ; P5D2), and VCAM-1 (HAE-2Z) from R&D Systems. Unconjugated antibodies to the $\alpha_4\beta_7$ integrin, namely Act-1 (mouse) and vedolizumab (humanized Act-1), and a humanized control antibody with a different antigen specificity but the same Fc IgG1 domain as vedolizumab, were available in-house, in addition to Alexa Fluor 647 conjugated vedolizumab or biotin-Act-1. Primary antibodies for the human tissue cross-reactivity investigation were rabbit anti-vedolizumab (generated in-house), anti- β_2 -microglobulin (Dako, Carpinteria, CA), and a negative control human IgG1 (Chemicon, Temecula, CA).

Cell Lines and Culture Media. The human B-cell lymphoma cell line, RPMI8866 (stably expressing $\alpha_4\beta_7$), was a kind gift from Dr David Erle (University of California, San

JPET #153973

Francisco). The human B-cell lymphoma cell line, RAMOS (stably expressing $\alpha_4\beta_1$, originally sourced from the American Type Culture Collection, Manassas, VA), and $\alpha_E\beta_7$ L1.2 cell-transfectants were generated in-house using cDNA provided by Christina Parker and Michael Brenner (Brigham and Women's Hospital, Boston, MA). Culture medium for RPMI8866 and RAMOS cell lines consisted of RPMI-1640 medium supplemented with 1% penicillin/streptomycin and 1% L-glutamine (all Invitrogen, Carlsbad, CA), and 10% US-defined fetal bovine serum (Hyclone, Logan, UT). Culture medium for $\alpha_E\beta_7$ transfectants consisted of RPMI-1640 medium supplemented with 1% penicillin/streptomycin, 1% sodium pyruvate, 1% L-glutamine, and 2 $\mu\text{g/ml}$ puromycin (all Invitrogen), 0.1% β -mercaptoethanol (Sigma-Aldrich, St. Louis, MO) and 10% US-defined fetal bovine serum (Hyclone).

Immunohistochemistry of Normal Human Tissues. The binding specificity of vedolizumab in 38 different types of normal human tissues (three independent donors per tissue type) was investigated by immunohistochemistry. The quality of these tissues was verified by robust staining with a positive-control antibody against β_2 -microglobulin (Dako, Carpinteria, CA). Sections (5 μm) were cut from fresh frozen tissue samples embedded in OCT Compound (Sakura Finetek USA, Inc., Torrance, CA) and fixed in acetone for 10 min at room temperature. Just prior to staining, slides were fixed for 10 s in 10% neutral buffered formalin. Acetone/formalin-fixed cryosections were rinsed twice in phosphate buffered saline (PBS) and incubated for 20 min with a protein block (PBS; 0.5% casein; 5% human gamma globulins; 0.02% goat IgG; 1 mg/ml heat-aggregated human IgG) designed to reduce nonspecific binding. Unconjugated vedolizumab or a negative control human IgG1 (Chemicon, Temecula, CA) were applied to sections at 2 or 20 $\mu\text{g/ml}$ and incubated at room temperature for one hour. The slides were then rinsed twice with PBS and an indirect immunoperoxidase procedure was performed to

JPET #153973

detect these primary reagents. The secondary antibody, rabbit anti-vedolizumab, was then applied at 5 µg/ml for 30 min and rinsed twice with PBS. Endogenous peroxidase was blocked by incubating the slides for 5 min with the peroxidase solution provided in the Dako EnVision+ Kit and then rinsing twice with PBS. The slides were then treated for 30 min with the peroxidase-labeled goat anti-rabbit IgG polymer supplied in the Dako EnVision+ Kit, then rinsed twice with PBS, and treated for 8 min with the substrate-chromogen (DAB+) solution supplied in the Dako EnVision+ Kit. All slides were rinsed with tap water, counterstained with hematoxylin, washed, 'blued' in saturated lithium carbonate, washed, dehydrated through alcohols, cleared in xylene, and coverslipped. Staining intensity was graded semi-quantitatively by a board-certified anatomic pathologist.

Staining of Cell Lines and Whole Blood. For the staining of cell lines, cells were resuspended at 2×10^6 /ml in FACS buffer (5% fetal bovine serum and 0.05% sodium azide in D-PBS (Dulbecco's phosphate buffers saline without calcium and magnesium); (VWR, West Chester, PA) and 200 µl samples were stained with the appropriate monoclonal antibodies (see *Proteins and Antibodies*) at 4°C for 30 min. Samples were washed with FACS buffer and analyzed by flow cytometry (FACSCalibur, BD). For the staining of human whole blood, 200 µl samples from healthy human volunteers were stained with the appropriate monoclonal antibody at 4°C for 30 min. Red blood cells were lysed with BD FACS lysing solution, and samples then washed with FACS buffer and analyzed by flow cytometry. In all cases, antibodies were used at saturating concentrations and, in many cases, up to four antibodies were used per sample. Appropriate single- or two-color control stains were also performed.

Saturation and Competitive Binding Analyses. The potency of vedolizumab binding to human leukocytes was examined through the generation of: 1) antibody saturation binding

JPET #153973

curves with labeled vedolizumab or Act-1, and 2) antibody binding competition curves for the competing binding of labeled antibody with unlabeled antibodies (vedolizumab, Act-1, or isotype control IgG). Experiments were performed in 96-well v-bottom plates (Corning Inc., Corning, NY). For saturation binding experiments and determination of EC_{50} values, 100 μ l of human peripheral blood from healthy human volunteers were incubated with the labeled antibody at the indicated range of concentrations in a final volume of 200 μ l. In these saturation experiments, at all concentrations tested, specific binding was demonstrated by competition with 20-fold molar excess of unlabeled antibody. For binding competition experiments, 100 μ l of human peripheral blood were incubated with the labeled antibody at its EC_{50} and the unlabeled antibody at the indicated range of concentrations in a final volume of 200 μ l. Plates were incubated at 4°C for 30min and cells were then washed. Red blood cells were lysed, washed, and stained with antibodies specific for memory $CD4^+$ T lymphocytes (CD4, CD45RO) and B lymphocytes (CD19). Binding to either memory $CD4^+$ T or B lymphocytes was examined by flow cytometry using a FACSCalibur flow cytometer and CellQuest Pro software. The geometric mean fluorescence intensity (GMFI) values of the positive memory $CD4^+$ T-lymphocyte population or the entire B lymphocyte population were plotted against antibody concentration. In binding competition experiments, GMFI data were plotted as percentage inhibition versus antibody concentration. EC_{50} (for saturation binding curves) or median inhibition concentration (IC_{50} ; for inhibition of binding curves) values were determined from these graphs using GraphPad Prism Version 4 nonlinear regression curve fits.

Intracellular Staining of Interleukin-17. Memory T-helper 17 (Th17) cells ($CD4^+CD45RO^+IL17A^+$) were identified from peripheral blood of normal donors. Peripheral blood mononuclear cells (PBMCs) were isolated from heparinized human blood by standard

JPET #153973

density-gradient procedures using Ficoll-Paque Plus (Amersham Biosciences, Piscataway, NJ). PBMCs were resuspended in assay buffer for CD4 memory cell interleukin (IL) 17A intracellular staining (eBioscience) according to the manufacturer's instructions. PBMCs were stimulated (or not stimulated, for the control samples) with 50 ng/ml phorbol 12-myristate 13-acetate (PMA; Sigma-Aldrich) and 1 μ g/ml Ionomycin (Sigma-Aldrich) in the presence of 3 μ M Monensin (Sigma-Aldrich) for 5 hours at 37°C. After washing, cells were stained with fluorescent-labeled antibodies: vedolizumab, anti- α 4 (CD49d; 9F10) and anti- β 7 (FIB504), anti-CD4 (SK3) and anti-CD45RO (UCHL1), where applicable, at 4°C for 30 min. Cells were then washed with cold PBS and resuspended in fixation and permeabilization working solution (eBioscience) staining buffer at 4°C for 30 min. After fixation and permeabilization, cells were washed with permeabilization buffer (eBioscience) and blocked with 10% normal rat serum at 4°C for 10 min. After the blocking step, cells were stained with fluorochrome conjugated anti-IL17A antibody (eBioscience) at 4°C for 30 min. Finally, cells were washed with permeabilization buffer and analyzed by flow cytometry in a FACSCalibur using CellQuest Pro software. The memory Th17 population was examined for expression of the α 4 β 7 integrin and the α 4 and β 7 chains. Some experiments were performed with isolated CD4⁺ memory T lymphocytes (Miltenyi Biotech, Auburn CA) with very similar results to those with PBMCs.

Adhesion Assays. For MAdCAM-1 and VCAM-1 experiments, 96-well ELISA plates (Thermo Fisher Scientific, Rochester, NY) were prepared 24 h in advance by coating with 100 μ l of 2 μ g/ml recombinant protein diluted in PBS at 4°C. For fibronectin experiments, commercially available precoated plates were used (see *Proteins and Antibodies*). On the assay day, the coating solution was removed before blocking with blocking buffer (0.5% bovine serum albumin [BSA], Sigma-Aldrich, in PBS) at 37°C (5% CO₂/95% O₂) for 1 h. Experiments on low-

JPET #153973

and high-affinity binding to integrins were performed in the absence or presence of Mn^{+2} , respectively; Mn^{+2} was added to induce the high-affinity conformation of the integrin. Assay buffer for low-affinity experiments was RPMI-1640, 0.1% BSA, 10 mM HEPES, pH 7, and for high-affinity experiments was 1 mM Mn^{2+} , Dulbecco's modified eagle medium (DMEM), 0.1% BSA, 10 mM HEPES, pH 7. For dose-dependent antibody inhibition curves, antibodies were diluted and cells resuspended in the indicated corresponding assay buffers for low- or high-affinity binding conditions. Premixed cell-antibody samples (100 μ l at 2×10^6 cells/ml) were added to the protein-coated plates after removal of the blocking buffer. Plates were incubated at 37°C (5% $CO_2/95\%$ O_2) for 1 h, washed 2 to 5 times with PBS, and adhered cells were detected by adding alamarBlue® (Trek Diagnostic Systems, Cleveland, OH). Plates were incubated at 37°C (5% $CO_2/95\%$ O_2) for 4 h and read by a fluorescence reader (Molecular Devices, Sunnyvale, CA). Experiments were performed in triplicate, included isotype control antibodies, and were repeated at least three times. Relative fluorescence units were plotted against antibody concentration and IC_{50} values were determined from these graphs using GraphPad Prism Version 4 nonlinear regression curve fits.

Inhibition of MAdCAM-1 Binding to $CD4^+$ Memory T-lymphocytes. Vedolizumab inhibition of high-affinity binding of MAdCAM-1 to human peripheral-blood memory $CD4^+$ T-lymphocytes was tested. Peripheral blood (90 μ l) was incubated with a saturating concentration (3 μ g/ml) of MAdCAM-1-murine-Fc fusion protein and 4 mM $MnCl_2$ in a final volume of 100 μ l for 1 h at room temperature, in the presence or absence of vedolizumab. This saturating concentration was determined from previous MAdCAM-1-Fc protein binding saturation curves with three independent donors. After washing with assay buffer (25 mM Tris, 4 mM $MnCl_2$, 2.7 mM KCl, 150 mM NaCl, 0.5% BSA, pH 7.2), the cells were stained with fluorescent-labeled

JPET #153973

anti-mouse IgG for 15 min at room temperature. After washing again, cells were incubated with mouse serum for 10 min at room temperature, followed by staining with anti-CD4 and anti-CD45RO antibodies for 15 min at room temperature. After washing, red blood cells were lysed with BD FACS lysing solution and analyzed by flow cytometry in a FACSCalibur using CellQuest Pro software. Antibody dose-dependent inhibition curves were obtained by plotting the percentage of memory CD4⁺ T-lymphocytes that bound MAdCAM-1 versus antibody concentration using GraphPad Prism Version 4. IC₅₀ values were determined from these graphs using GraphPad Prism Version 4 nonlinear regression curve fits.

JPET #153973

Results

Binding of Vedolizumab to Human Tissue *Ex Vivo*. The binding specificity of vedolizumab was investigated in 38 different types of normal human tissue by immunohistochemistry. Binding of vedolizumab was restricted to the cell membrane of mononuclear cells in lymphoid tissues, mononuclear infiltrates in tissues of the GI tract and bladder, and mononuclear cells in the lumens of blood vessels (Table 1). In GI tract tissues, vedolizumab bound mononuclear cells organized in submucosal lymphoid nodules and/or scattered in lamina propria. The large and small intestine contained the highest frequency of mononuclear cells that were bound by vedolizumab (data not shown).

Binding Specificity of Vedolizumab to Human Leukocytes *Ex Vivo*. Flow cytometry experiments were performed on human peripheral blood stained with vedolizumab or Act-1, anti- α_4 and anti- β_1 monoclonal antibodies (mAbs), and markers of leukocyte subsets (including memory and naïve CD4 and CD8 T lymphocytes, B lymphocytes, natural killer cells, monocytes, basophils, eosinophils, and neutrophils). Experiments were designed so that coexpression of the $\alpha_4\beta_1$ and $\alpha_4\beta_7$ integrins and binding of vedolizumab to subsets expressing the $\alpha_4\beta_1$ integrin could also be examined. Vedolizumab bound to the majority of B lymphocytes, naïve CD4 and CD8 T lymphocytes, natural killer cells, and basophils at low to intermediate levels (Fig. 1, A and B). Vedolizumab bound to B lymphocytes at intermediate levels uniformly, to natural killer cells and basophils at low levels uniformly, and to naïve CD4 and CD8 T lymphocytes from low to intermediate levels. Vedolizumab bound to approximately 25% of the memory (CD45RO⁺) CD4⁺ T lymphocytes at high levels ($\alpha_4\beta_7^{\text{hi}}$) and to 5 to 10% at intermediate levels, and not to the rest of the population (Fig. 1, A and B, and Fig. 2A). Vedolizumab bound to the majority of the

JPET #153973

naïve (CD45RO⁻) CD4⁺ and CD8⁺ T lymphocytes, and to approximately 50% of the memory (CD45RO⁺) CD8⁺ T lymphocytes, at low to intermediates levels (Fig. 1, A and B, and Fig. 2A). Vedolizumab bound to all eosinophils at intermediate to high levels, and to approximately 15% of monocytes at low levels, but did not bind to neutrophils (Fig. 1, A and B). The highest level of binding by vedolizumab was observed on the $\alpha_4\beta_7^{\text{hi}}$ population of memory CD45RO⁺ CD4⁺ T lymphocytes (Fig. 1B). The specificity of binding to the $\alpha_4\beta_7$ integrin by vedolizumab was verified by competition with Act-1; unlabeled Act-1 completely inhibited binding of vedolizumab on all leukocyte subsets examined (data not shown). The same antigen specificity between these two antibodies was also demonstrated by the complete inhibition of labeled Act-1 binding to all leukocytes exposed to unlabeled vedolizumab.

The binding profile of vedolizumab contrasts the expression profile of the $\alpha_4\beta_1$ integrin. Expression of the $\alpha_4\beta_1$ integrin was generally more widespread than binding by vedolizumab. Vedolizumab bound naïve CD4⁺ T lymphocytes at varying levels (Fig. 2A), whereas these cells expressed the $\alpha_4\beta_1$ integrin uniformly (Fig. 2B). Vedolizumab bound to a specific subset of the memory CD4⁺ T lymphocyte population; vedolizumab bound approximately 25% of memory CD4⁺ T lymphocytes at high levels (Fig. 2A), whereas most of these cells expressed relatively high levels of the α_4 and/or β_1 chains (Fig. 2B). Three major subsets of memory CD4⁺ T lymphocytes can be defined by $\alpha_4\beta_1$ integrin expression: α_4^- , $\alpha_4^{\text{hi}}\beta_1^{\text{hi}}$, and $\alpha_4^{\text{hi}}\beta_1^{\text{lo}}$. Vedolizumab binds to most (~80%) of the $\alpha_4^{\text{hi}}\beta_1^{\text{lo}}$ T helper lymphocytes at high levels (Fig. 2C); this is the subset that contains the majority of the $\alpha_4\beta_7^{\text{hi}}$ subset. In contrast, the majority (~90%) of $\alpha_4^{\text{hi}}\beta_1^{\text{hi}}$ and all $\alpha_4^{\text{lo}}\beta_1^{\text{hi}}$ T helper lymphocytes are not bound by vedolizumab (Fig. 2C). Similarly, a majority (~85%) of monocytes are not bound by vedolizumab (Fig. 2, D and E), but express relatively high levels of the $\alpha_4\beta_1$ integrin (Fig. 2F).

JPET #153973

Vedolizumab Specificity for the $\alpha_4\beta_7$ Integrin Versus the $\alpha_4\beta_1$ and $\alpha_E\beta_7$ Integrins.

The specificity of vedolizumab binding for the integrin $\alpha_4\beta_7$ versus $\alpha_4\beta_1$ in whole blood is illustrated by comparing two subsets of leukocytes that express high levels of the $\alpha_4\beta_1$ integrin but do not bind vedolizumab, specifically the $\alpha_4\beta_1^{\text{hi}}$ subset of the memory CD4 population (Fig. 2B, plot 1, quadrant II) and monocytes (Fig. 2F). Vedolizumab did not bind the vast majority of cells in either $\alpha_4\beta_1^{\text{hi}}$ populations (Fig. 2C plot II and Fig. 2D, respectively). The lack of binding by vedolizumab was maintained up to a concentration of 400 $\mu\text{g/ml}$ (data not shown). The analysis of the specificity of vedolizumab for the $\alpha_4\beta_7$ integrin versus $\alpha_E\beta_7$ in whole blood by flow cytometry was not possible because all the $\alpha_E\beta_7$ -expressing cells are contained within the $\alpha_4\beta_7^{\text{hi}}$ subset. The specificity of binding to integrins containing the α_4 and/or β_7 chains by vedolizumab was investigated further with cell lines expressing the $\alpha_4\beta_1$, $\alpha_4\beta_7$, or $\alpha_E\beta_7$ integrins exclusively. Vedolizumab bound to RPMI8866 cells (Fig. 3A) that expressed the α_4 and β_7 chains (Fig. 3B) but not the β_1 or α_E chains (not shown). Incubation with Act-1 competed with the binding of vedolizumab to RPMI8866 cells, confirming the specificity of binding to the $\alpha_4\beta_7$ integrin (data not shown). Vedolizumab did not bind to RAMOS cells (Fig. 3C) that expressed the α_4 and β_1 chains (Fig. 3D) but not the β_7 chain (data not shown), nor to mouse L1.2 cell transfectants (Fig. 3E) that expressed the human α_E and β_7 chains (Fig. 3, E and F), but not the human α_4 chain (data not shown).

Characterization of the Memory CD4 T Lymphocyte Population for Expression of the $\alpha_4\beta_1$ and $\alpha_4\beta_7$ Integrins and IL-17. A subset (~20%) of the Th17 cell population in peripheral blood was bound by vedolizumab (Fig. 4), and similar data were obtained for expression of the β_7 chain (data not shown). In contrast, the majority (80%) of the memory Th17

JPET #153973

cell population expressed the α_4 chain ($\alpha_4^+\beta_1^+$ and $\alpha_4^+\beta_7^+$; Fig. 4). The Th17 cell population therefore consists of three major subsets: α_4^- (20%), $\alpha_4\beta_1^{\text{hi}}$ (60%), and $\alpha_4\beta_7^{\text{hi}}$ (20%).

Potency of Binding of Vedolizumab to B and Memory CD4⁺ T Lymphocytes. The potency of vedolizumab for binding to human peripheral-blood B and memory CD4⁺ lymphocytes was estimated from saturation binding curves in experiments with labeled vedolizumab (Fig. 5A). The EC₅₀ values were 0.067 $\mu\text{g/ml}$ (0.4 nM) and 0.042 $\mu\text{g/ml}$ (0.3 nM) for B and memory CD4⁺ lymphocytes, respectively. The potency of vedolizumab for binding to human peripheral-blood B and memory CD4⁺ lymphocytes was also estimated from competitive binding experiments in which binding of labeled vedolizumab at its EC₅₀ was competed off by unlabeled vedolizumab (Fig. 5B). The mean IC₅₀ values were 0.045 $\mu\text{g/ml}$ (0.3 nM) and 0.044 $\mu\text{g/ml}$ (0.3 nM) for B and memory CD4⁺ lymphocytes, respectively. Similar results were obtained with Act-1; the IC₅₀ values for Act-1 binding were 0.062 $\mu\text{g/ml}$ (0.010 nM) and 0.059 $\mu\text{g/ml}$ (0.008 nM) for B and memory CD4⁺ lymphocytes, respectively (data not shown).

Vedolizumab Inhibits Adhesion of $\alpha_4\beta_7^+$ Cells to MAdCAM-1 and Fibronectin But Not to VCAM-1. The neutralizing potency and specificity of vedolizumab was determined in cell adhesion assays with $\alpha_4\beta_7$ -expressing RPMI8866 cells and the cell adhesion proteins, MAdCAM-1, VCAM-1, and the alternatively spliced form of fibronectin containing the CS-1 peptide. Vedolizumab inhibited high-affinity adhesion of $\alpha_4\beta_7$ -expressing RPMI8866 cells (Mn²⁺-activated) to MAdCAM-1 (Fig. 6A) with a mean IC₅₀ value of $0.058 \pm 0.024 \mu\text{g/ml}$ ($0.39 \pm 0.16 \text{ nM}$; n = 6). Vedolizumab inhibited low-affinity adhesion of $\alpha_4\beta_7$ -expressing RPMI8866 cells (no Mn²⁺ activation) to MAdCAM-1 with similar potency ($0.023 \pm 0.012 \mu\text{g/ml}$; $0.15 \pm 0.08 \text{ nM}$; n = 7; Fig. 6B). Vedolizumab inhibited adhesion of $\alpha_4\beta_7$ -expressing RPMI8866 cells to fibronectin (Mn²⁺-activated, as required for fibronectin binding; Fig. 6F) with a mean IC₅₀ value

JPET #153973

of 0.02 ± 0.012 $\mu\text{g/ml}$ (0.14 ± 0.08 nM; $n = 4$). In contrast, vedolizumab did not inhibit adhesion of $\alpha_4\beta_7$ -expressing RPMI8866 cells to VCAM-1 under high- (Fig. 6C, $n = 4$, and Fig. 6E) or low-affinity (Fig. 6D, $n = 3$, and Fig. 6E) states, even at 400 $\mu\text{g/ml}$, the highest concentration tested (Fig. 6E, $n = 3$). The anti- α_4 mAb, in contrast, inhibited all adhesion of $\alpha_4\beta_7$ -expressing RPMI8866 cells with MAdCAM-1, VCAM-1, and fibronectin with subnanomolar potency (Fig. 6, A–F). The humanized mAb negative control (Fig. 6, A, B, and F) and the murine isotype-matched negative control (Fig. 6, A–F) had no effect on adhesion. The effect of vedolizumab on the binding of MAdCAM-1 to T lymphocytes in human whole blood was also evaluated by flow cytometry. Vedolizumab inhibited the binding of soluble human MAdCAM-1-Fc fusion protein to the $\alpha_4\beta_7^{\text{hi}}$ CD4 memory cell population with similar potency ($\text{IC}_{50} = 0.034$ $\mu\text{g/ml}$, 0.225 nM mean of three donors) (Fig. 7).

Vedolizumab Has No Effect on Adhesion of the $\alpha_4\beta_1$ Integrin to VCAM-1 or Fibronectin. The specificity of vedolizumab was further characterized in adhesion assays with the $\alpha_4\beta_1$ -expressing RAMOS cells. Vedolizumab did not inhibit high- (Mn^{2+} -activated) or low-affinity (no Mn^{2+}) adhesion of $\alpha_4\beta_1$ -expressing RAMOS cells to VCAM-1 (Fig. 8, A and C, respectively), even at the highest concentrations assayed, 400 $\mu\text{g/ml}$ (Fig. 8, B and D, respectively). Conversely, anti- α_4 mAb, anti- β_1 mAb, and a combination thereof, inhibited all adhesion between $\alpha_4\beta_1$ -expressing RAMOS cells and VCAM-1 (Fig. 8, A–D). Vedolizumab did not inhibit adhesion of $\alpha_4\beta_1$ -expressing RAMOS cells to fibronectin at 400 $\mu\text{g/ml}$, the highest concentration assayed, whereas a combination of anti- α_4 and anti- β_1 mAbs inhibited adhesion (Fig. 8E). RAMOS cells did not bind to MAdCAM-1, even after integrin activation with Mn^{2+} (data not shown).

JPET #153973

Discussion

Infiltration of the GI tract by T lymphocytes is a pathogenic mechanism of UC and CD (Xavier and Podolsky, 2007). Migration into the GI tract is a complex, multi-step process requiring the coordinated interaction of several adhesion and signaling molecules (selectins, integrins, chemokine receptors) on the surface of T-lymphocytes, with their corresponding ligands on the endothelium (Salmi and Jalkanen, 2005). The $\alpha_4\beta_7$ integrin is a pivotal mediator of infiltration of GI tract by T lymphocytes and antagonizing its adhesion to MAdCAM-1 provides efficacy in animal models of IBD (Hesterberg et al., 1996; Picarella et al., 1997) and in patients with UC (Feagan et al., 2005; Feagan et al., 2008) and CD (Feagan et al., 2005; Feagan et al., 2008). These investigations also demonstrated that antagonizing the $\alpha_4\beta_7$ integrin is well tolerated. The absence of overt deleterious effects is partially attributable to vedolizumab binding exclusively to leukocytes. This binding profile is consistent with the expression profile of the human $\alpha_4\beta_7$ integrin (Schweighoffer et al., 1993; Erle et al., 1994; Farstad et al., 1997; Rott et al., 2000).

This desirable profile encouraged targeting the $\alpha_4\beta_7$ integrin by three different therapeutic strategies. One of these strategies targets the β_7 chain of the integrin and, consequently, inhibits both the $\alpha_4\beta_7$ and $\alpha_E\beta_7$ adhesion pathways thereby inhibiting the localization and retention of T lymphocytes within epithelial layers in numerous tissues (Kilshaw, 1999). This could potentially elicit systemic effects, perturbing immunosurveillance of healthy epithelial tissue and reducing inflammation in diseased tissue. The second strategy targets the α_4 chain and inhibits both the $\alpha_4\beta_7$ and $\alpha_4\beta_1$ integrins. The $\alpha_4\beta_1$ integrin is expressed by all leukocytes except neutrophils (Gonzalez-Amaro et al., 2005), and antagonism by

JPET #153973

natalizumab inhibits adhesion of the $\alpha_4\beta_1$ integrin to VCAM-1, fibronectin, and osteopontin, and the adhesion of the $\alpha_4\beta_7$ integrin to MAdCAM-1, VCAM-1 and fibronectin (Biogen Idec, 2006). The $\alpha_4\beta_1$ integrin mediates adhesion in many different types of tissue, and inhibition by natalizumab therefore induces diverse systemic effects, such as mobilization of hematopoietic progenitor cells from the bone marrow (Bonig et al., 2008; Zohren et al., 2008), leukocytosis in the vasculature (Ghosh et al., 2003; Sandborn et al., 2005; Targan et al., 2007), and decreases in the number of leukocytes in cerebral spinal fluid (Stuve et al., 2006a; Stuve et al., 2006b) and cerebral tissue (del Pilar Martin et al., 2008). This diverse profile of physiologic effects may confer efficacy in pathologically distinct diseases, such as multiple sclerosis (Miller et al., 2003) and CD (Ghosh et al., 2003; Sandborn et al., 2005; Targan et al., 2007). Repeated administration of natalizumab to multiple sclerosis and CD patients is, however, also associated with systemic immunosuppression, including an increased incidence of the fatal infectious disease, PML (Kleinschmidt-DeMasters and Tyler, 2005; Langer-Gould et al., 2005; Van Assche et al., 2005). It is postulated that the anti-inflammatory mechanism that mediate efficacy of natalizumab in multiple sclerosis and CD may also predispose patients to PML by decreasing immunosurveillance in the central nervous system (Berger and Houff, 2006; Stuve et al., 2006a; Stuve et al., 2006b; del Pilar Martin et al., 2008). Natalizumab may prevent the entry of memory T lymphocytes into the brain and perhaps into sites of viral latency, thereby precluding T lymphocytes from clearing or suppressing the viral infection (Berger, 2006; Stuve et al., 2006b; del Pilar Martin et al., 2008).

Vedolizumab utilizes a third strategy: exclusive targeting of the $\alpha_4\beta_7$ integrin.

Vedolizumab binds to the $\alpha_4\beta_7$ integrin, but not to the $\alpha_4\beta_1$ or $\alpha_E\beta_7$ integrins (Fig. 2 and 3). This specificity was confirmed in functional assays demonstrating that vedolizumab inhibits adhesion

JPET #153973

of $\alpha_4\beta_7$ -expressing cells exclusively (Fig. 6 and 7), but not of $\alpha_4\beta_1$ -expressing cells exclusively (Fig. 8). These data agree with immunoprecipitation experiments utilizing Act-1 (Schweighoffer et al., 1993). Specifically targeting the $\alpha_4\beta_7$ integrin enables vedolizumab to immunomodulate the GI tract without systemic effects, owing to the GI-specific role of the $\alpha_4\beta_7$ integrin in mediating infiltration by leukocytes (Butcher et al., 1999; Engelhardt and Briskin, 2005; Agace, 2006). This strategy does not elicit leukocytosis in UC and CD patients, and has demonstrated an excellent clinical safety profile to date (Feagan et al., 2005; Feagan et al., 2008).

Another component of the unique pharmacologic activity of vedolizumab could be selective inhibition of cellular activity. Vedolizumab selectively inhibits the adhesion of cells expressing the $\alpha_4\beta_7$ integrin to MAdCAM-1 and fibronectin, but not to VCAM-1 (Fig. 6 and 7). These data are consistent with qualitative reports for the effect of Act-1 on adhesion of B and T lymphocytes to these ligands (Postigo et al., 1993; Schweighoffer et al., 1993; Erle et al., 1994; Walsh et al., 1996).

Differences in expression of α_4 chains between memory $CD4^+$ T lymphocytes also contribute to the unique clinical profile of vedolizumab. Circulating effector memory $CD4^+$ T lymphocytes can be divided into three subpopulations according to expression of the α_4 chain: 1) 20% that do not express the α_4 chain (Fig. 2B); 2) 50% that express high levels of α_4 and β_1 chains (Fig. 2B) that would be bound by an anti- α_4 therapeutic but not by vedolizumab (Fig. 2C), and 3) 30% that express high levels of the $\alpha_4\beta_7$ integrin and low levels of the β_1 chain (Fig. 2C) that would be bound by both an anti- α_4 therapeutic and vedolizumab. The $CD4^+$ memory $\alpha_4\beta_7^{hi}$ population is postulated to be pathogenic in IBD (Butcher et al., 1999; Salmi and Jalkanen, 2005), and the clinical efficacy of natalizumab in CD and vedolizumab in CD and UC buttress this paradigm (Ghosh et al., 2003; Feagan et al., 2005; Sandborn et al., 2005; Feagan et

JPET #153973

al., 2008). Vedolizumab specifically targets the CD4⁺ memory subpopulation that is pathogenic in IBD ($\alpha_4\beta_7^{\text{hi}}$), while sparing other CD4⁺ memory subpopulations ($\alpha_4\beta_1^{\text{hi}}$) and monocytes (Fig. 2) that are integral for immunosurveillance and host defense.

We discovered that vedolizumab binds to a subset (~20%) of Th17 cells that express the gut-tropic $\alpha_4\beta_7^{\text{hi}}$ phenotype (Fig. 4). This pro-inflammatory subset is found in numerous types of inflamed tissue and is postulated to mediate many different autoimmune diseases, such as psoriasis, psoriatic arthritis, rheumatoid arthritis, type 1 diabetes, transplant rejection, and tumor immunotherapy (Iwakura and Ishigame, 2006). IL-23 plays an important role in the maintenance and function of the Th17 subset of CD4 memory T lymphocytes. Single nucleotide polymorphisms of the human IL-23 receptor gene are associated with increased risk and protection from CD (Duerr et al., 2006). Ustekinumab is a therapeutic antibody targeting the human p40 subunit of the IL-12 and IL-23 cytokines, and is efficacious in CD (Sandborn et al., 2008) and psoriasis (Leonardi et al., 2008; Papp et al., 2008). It appears that vedolizumab targets only a subset (20%) of the Th17 cells, namely the GI-tropic, $\alpha_4\beta_7^{\text{hi}}$ subset and thus could provide efficacy in IBD more specifically than ustekinumab, conferring an improved clinical risk-to-benefit profile in patients with IBD.

Targeting systemic mediators of inflammation, such as $\alpha_4^{\text{hi}}\beta_1^{\text{hi}}$ T cells and Th17 cells, inhibits systemic immunosurveillance, which may predispose patients to infection and/or neoplasia (Engelhardt and Briskin, 2005; Ransohoff, 2005; Iwakura and Ishigame, 2006; Wei et al., 2006; Mottet and Golshayan, 2007). The role of the $\alpha_4\beta_7$ integrin in immunosurveillance, in contrast, is restricted to the GI tract (Butcher et al., 1999; Salmi and Jalkanen, 2005; Agace, 2006). Gut-specific immunomodulation by vedolizumab is hence less likely to predispose patients to infection and/or neoplasia outside of the GI-tract than by anti- α_4 , anti- β_7 , and anti-

JPET #153973

p40 (IL-12/IL-23) subunit therapeutics. The specificity of vedolizumab for GI-tropic T lymphocytes offers clinical efficacy in IBD (Feagan et al., 2005; Feagan et al., 2008) without some of the undesirable systemic effects characteristic of natalizumab and ustekinumab. The ability to modulate inflammation specifically within the GI tract, without systemic immunosuppression, is likely to confer efficacy in IBD with an improved safety profile and risk-to-benefit ratio.

JPET #153973

Acknowledgments

The authors would like to acknowledge the following people for insightful discussions and review of the manuscript: Irving Fox, M.D., Asit Parikh, M.D., Ph.D., Carl Alden, D.V.M., Veit Schmelmer, Jennifer Elliot, Ph.D., Karen Repetny, Brad Nohe, Charles Baum, MD, Gretchen Bodun, Betsy Pilmer, Yasushi Shimizu, Teruhisa Tanaka, Kenichiro Nogami, Ohta Sunao, Shaila Basavappa, and Yasuko Tokifuji.

JPET #153973

References

- Agace WW (2006) Tissue-tropic effector T cells: generation and targeting opportunities. *Nature Reviews. Immunology* **6**:682-692.
- Berger JR (2006) Natalizumab and progressive multifocal leucoencephalopathy. *Annals of the Rheumatic Diseases* **65 Suppl 3**:iii48-53.
- Berger JR and Houff S (2006) Progressive multifocal leukoencephalopathy: lessons from AIDS and natalizumab. *Neurological Research* **28**:299-305.
- Berger JR and Koralknik IJ (2005) Progressive multifocal leukoencephalopathy and natalizumab--unforeseen consequences. *New England Journal of Medicine* **353**:414-416.
- Biogen Idec I (2006) TYSABRI® (natalizumab), in, Biogen Idec Inc., Cambridge, MA.
- Bonig H, Wundes A, Chang KH, Lucas S and Papayannopoulou T (2008) Increased numbers of circulating hematopoietic stem/progenitor cells are chronically maintained in patients treated with the CD49d blocking antibody natalizumab. *Blood* **111**:3439-3441.
- Butcher EC and Picker LJ (1996) Lymphocyte homing and homeostasis. *Science* **272**:60-66.
- Butcher EC, Williams M, Youngman K, Rott L and Briskin M (1999) Lymphocyte trafficking and regional immunity. *Advances in Immunology* **72**:209-253.
- del Pilar Martin M, Cravens PD, Winger R, Frohman EM, Racke MK, Eagar TN, Zamvil SS, Weber MS, Hemmer B, Karandikar NJ, Kleinschmidt-DeMasters BK and Stuve O (2008)

JPET #153973

Decrease in the numbers of dendritic cells and CD4+ T cells in cerebral perivascular spaces due to natalizumab. *Arch Neurol* **65**:1596-1603.

Duerr RH, Taylor KD, Brant SR, Rioux JD, Silverberg MS, Daly MJ, Steinhart AH, Abraham C, Regueiro M, Griffiths A, Dassopoulos T, Bitton A, Yang H, Targan S, Datta LW, Kistner EO, Schumm LP, Lee AT, Gregersen PK, Barmada MM, Rotter JI, Nicolae DL and Cho JH (2006) A genome-wide association study identifies IL23R as an inflammatory bowel disease gene. *Science* **314**:1461-1463.

Engelhardt B and Briskin MJ (2005) Therapeutic targeting of alpha 4-integrins in chronic inflammatory diseases: tipping the scales of risk towards benefit? *European Journal of Immunology* **35**:2268-2273.

Engelhardt B, Laschinger M, Schulz M, Samulowitz U, Vestweber D and Hoch G (1998) The development of experimental autoimmune encephalomyelitis in the mouse requires alpha4-integrin but not alpha4beta7-integrin. *Journal of Clinical Investigation* **102**:2096-2105.

Erle DJ, Briskin MJ, Butcher EC, Garcia-Pardo A, Lazarovits AI and Tidswell M (1994) Expression and function of the MAdCAM-1 receptor, integrin alpha 4 beta 7, on human leukocytes. *Journal of Immunology* **153**:517-528.

Farstad IN, Halstensen TS, Kvale D, Fausa O and Brandtzaeg P (1997) Topographic distribution of homing receptors on B and T cells in human gut-associated lymphoid tissue: relation of L-selectin and integrin alpha 4 beta 7 to naive and memory phenotypes. *American Journal of Pathology* **150**:187-199.

JPET #153973

Feagan BG, Greenberg GR, Wild G, Fedorak RN, Pare P, McDonald JW, Cohen A, Bitton A, Baker J, Dube R, Landau SB, Vandervoort MK and Parikh A (2008) Treatment of active Crohn's disease with MLN0002, a humanized antibody to the alpha4beta7 integrin. *Clinical Gastroenterology and Hepatology* **6**:1370-1377.

Feagan BG, Greenberg GR, Wild G, Fedorak RN, Pare P, McDonald JW, Dube R, Cohen A, Steinhart AH, Landau S, Aguzzi RA, Fox IH and Vandervoort MK (2005) Treatment of ulcerative colitis with a humanized antibody to the alpha4beta7 integrin. *New England Journal of Medicine* **352**:2499-2507.

Ghosh S, Goldin E, Gordon FH, Malchow HA, Rask-Madsen J, Rutgeerts P, Vyhnaek P, Zadorova Z, Palmer T, Donoghue S and Natalizumab Pan-European Study G (2003) Natalizumab for active Crohn's disease. *New England Journal of Medicine* **348**:24-32.

Gonzalez-Amaro R, Mittelbrunn M and Sanchez-Madrid F (2005) Therapeutic anti-integrin (alpha4 and alphaL) monoclonal antibodies: two-edged swords? *Immunology* **116**:289-296.

Hesterberg PE, Winsor-Hines D, Briskin MJ, Soler-Ferran D, Merrill C, Mackay CR, Newman W and Ringler DJ (1996) Rapid resolution of chronic colitis in the cotton-top tamarin with an antibody to a gut-homing integrin alpha 4 beta 7. *Gastroenterology* **111**:1373-1380.

Iwakura Y and Ishigame H (2006) The IL-23/IL-17 axis in inflammation. *Journal of Clinical Investigation* **116**:1218-1222.

JPET #153973

Kilshaw PJ (1999) Alpha E beta 7. *Molecular Pathology* **52**:203-207.

Kleinschmidt-DeMasters BK and Tyler KL (2005) Progressive multifocal leukoencephalopathy complicating treatment with natalizumab and interferon beta-1a for multiple sclerosis. *New England Journal of Medicine* **353**:369-374.

Koralnik IJ (2006) Progressive multifocal leukoencephalopathy revisited: Has the disease outgrown its name? *Annals of Neurology* **60**:162-173.

Langer-Gould A, Atlas SW, Green AJ, Bollen AW and Pelletier D (2005) Progressive multifocal leukoencephalopathy in a patient treated with natalizumab. *New England Journal of Medicine* **353**:375-381.

Lazarovits AI, Moscicki RA, Kurnick JT, Camerini D, Bhan AK, Baird LG, Erikson M and Colvin RB (1984) Lymphocyte activation antigens. I. A monoclonal antibody, anti-Act I, defines a new late lymphocyte activation antigen. *Journal of Immunology* **133**:1857-1862.

Leonardi CL, Kimball AB, Papp KA, Yeilding N, Guzzo C, Wang Y, Li S, Dooley LT, Gordon KB and investigators Ps (2008) Efficacy and safety of ustekinumab, a human interleukin-12/23 monoclonal antibody, in patients with psoriasis: 76-week results from a randomised, double-blind, placebo-controlled trial (PHOENIX 1). *Lancet* **371**:1665-1674.

Miller DH, Khan OA, Sheremata WA, Blumhardt LD, Rice GP, Libonati MA, Willmer-Hulme AJ, Dalton CM, Miszkiel KA, O'Connor PW and International Natalizumab Multiple

JPET #153973

- Sclerosis Trial G (2003) A controlled trial of natalizumab for relapsing multiple sclerosis. *New England Journal of Medicine* **348**:15-23.
- Mottet C and Golshayan D (2007) CD4+CD25+Foxp3+ regulatory T cells: from basic research to potential therapeutic use. *Swiss Medical Weekly* **137**:625-634.
- Niino M, Bodner C, Simard ML, Alatab S, Gano D, Kim HJ, Trigueiro M, Racicot D, Guerette C, Antel JP, Fournier A, Grand'Maison F and Bar-Or A (2006) Natalizumab effects on immune cell responses in multiple sclerosis. *Annals of Neurology* **59**:748-754.
- Papp KA, Langley RG, Lebwohl M, Krueger GG, Szapary P, Yeilding N, Guzzo C, Hsu MC, Wang Y, Li S, Dooley LT, Reich K and investigators Ps (2008) Efficacy and safety of ustekinumab, a human interleukin-12/23 monoclonal antibody, in patients with psoriasis: 52-week results from a randomised, double-blind, placebo-controlled trial (PHOENIX 2). *Lancet* **371**:1675-1684.
- Picarella D, Hurlbut P, Rottman J, Shi X, Butcher E and Ringler DJ (1997) Monoclonal antibodies specific for beta 7 integrin and mucosal addressin cell adhesion molecule-1 (MAdCAM-1) reduce inflammation in the colon of scid mice reconstituted with CD45RB^{high} CD4⁺ T cells. *Journal of Immunology* **158**:2099-2106.
- Postigo AA, Sanchez-Mateos P, Lazarovits AI, Sanchez-Madrid F and de Landazuri MO (1993) Alpha 4 beta 7 integrin mediates B cell binding to fibronectin and vascular cell adhesion molecule-1. Expression and function of alpha 4 integrins on human B lymphocytes. *Journal of Immunology* **151**:2471-2483.

JPET #153973

Ransohoff RM (2005) Natalizumab and PML. *Nature Neuroscience* **8**:1275.

Rott LS, Briskin MJ and Butcher EC (2000) Expression of alpha4beta7 and E-selectin ligand by circulating memory B cells: implications for targeted trafficking to mucosal and systemic sites. *Journal of Leukocyte Biology* **68**:807-814.

Salmi M and Jalkanen S (2005) Lymphocyte homing to the gut: attraction, adhesion, and commitment. *Immunol Rev* **206**:100-113.

Sandborn WJ, Colombel JF, Enns R, Feagan BG, Hanauer SB, Lawrance IC, Panaccione R, Sanders M, Schreiber S, Targan S, van Deventer S, Goldblum R, Despain D, Hogge GS, Rutgeerts P, International Efficacy of Natalizumab as Active Crohn's Therapy Trial G and Evaluation of Natalizumab as Continuous Therapy Trial G (2005) Natalizumab induction and maintenance therapy for Crohn's disease. *New England Journal of Medicine* **353**:1912-1925.

Sandborn WJ, Feagan BG, Fedorak RN, Scherl E, Fleisher MR, Katz S, Johanns J, Blank M and Rutgeerts P (2008) A Randomized Trial of Ustekinumab, a Human Interleukin-12/23 Monoclonal Antibody, in Patients With Moderate-to-Severe Crohn's Disease. *Gastroenterology* **135**:1130-1141.

Schweighoffer T, Tanaka Y, Tidswell M, Erle DJ, Horgan KJ, Luce GE, Lazarovits AI, Buck D and Shaw S (1993) Selective expression of integrin alpha 4 beta 7 on a subset of human CD4+ memory T cells with Hallmarks of gut-tropism. *Journal of Immunology* **151**:717-729.

JPET #153973

Stuve O, Marra CM, Bar-Or A, Niino M, Cravens PD, Cepok S, Frohman EM, Phillips JT, Arendt G, Jerome KR, Cook L, Grand'Maison F, Hemmer B, Monson NL and Racke MK (2006a) Altered CD4⁺/CD8⁺ T-cell ratios in cerebrospinal fluid of natalizumab-treated patients with multiple sclerosis. *Archives of Neurology* **63**:1383-1387.

Stuve O, Marra CM, Jerome KR, Cook L, Cravens PD, Cepok S, Frohman EM, Phillips JT, Arendt G, Hemmer B, Monson NL and Racke MK (2006b) Immune surveillance in multiple sclerosis patients treated with natalizumab. *Annals of Neurology* **59**:743-747.

Targan SR, Feagan BG, Fedorak RN, Lashner BA, Panaccione R, Present DH, Spehlmann ME, Rutgeerts PJ, Tulassay Z, Volfova M, Wolf DC, Hernandez C, Bornstein J, Sandborn WJ and International Efficacy of Natalizumab in Crohn's Disease Response and Remission Trial G (2007) Natalizumab for the treatment of active Crohn's disease: results of the ENCORE Trial. *Gastroenterology* **132**:1672-1683.

Tidswell M, Pachynski R, Wu SW, Qiu SQ, Dunham E, Cochran N, Briskin MJ, Kilshaw PJ, Lazarovits AI, Andrew DP, Butcher EC, Yednock TA and Erle DJ (1997) Structure-function analysis of the integrin beta 7 subunit: identification of domains involved in adhesion to MAdCAM-1. *Journal of Immunology* **159**:1497-1505.

Van Assche G, Van Ranst M, Sciot R, Dubois B, Vermeire S, Noman M, Verbeeck J, Geboes K, Robberecht W and Rutgeerts P (2005) Progressive multifocal leukoencephalopathy after natalizumab therapy for Crohn's disease. *New England Journal of Medicine* **353**:362-368.

JPET #153973

Walsh GM, Symon FA, Lazarovics AL and Wardlaw AJ (1996) Integrin alpha 4 beta 7 mediates human eosinophil interaction with MAdCAM-1, VCAM-1 and fibronectin. *Immunology* **89**:112-119.

Wei S, Kryczek I and Zou W (2006) Regulatory T-cell compartmentalization and trafficking. *Blood* **108**:426-431.

Xavier RJ and Podolsky DK (2007) Unravelling the pathogenesis of inflammatory bowel disease. *Nature* **448**:427-434.

Zohren F, Toutzaris D, Klarner V, Hartung HP, Kieseier B and Haas R (2008) The monoclonal anti-VLA-4 antibody natalizumab mobilizes CD34+ hematopoietic progenitor cells in humans. *Blood* **111**:3893-3895.

JPET #153973

Footnotes

a) Source of financial support

These investigations were supported by Millennium Pharmaceuticals Inc.

b) Previous presentation

Some of the data has been presented at the 2008 Advances in Inflammatory Bowel Diseases Crohn's and Colitis Foundation's Clinical and Research Conference and at the 4th Congress of ECCO, The European Crohn's and Colitis Organisation.

c) Reprint requests

Eric R. Fedyk, Ph.D.

Millennium Pharmaceuticals Inc.

40 Landsdowne Street

Cambridge, MA 02139

USA

E-mail: fedyk@mpi.com

JPET #153973

Legends for Figures

Fig. 1. Binding specificity of vedolizumab to human leukocytes. Human peripheral blood was stained with vedolizumab and antibodies specific for the various leukocyte subsets and examined by flow cytometry. (A) Flow cytometry plots illustrating vedolizumab binding to various subsets of leukocytes, identified by gating on the appropriate cellular markers. Vedolizumab binding is plotted against forward scatter, with the horizontal line indicating the level of background signal as determined from a negative control antibody. Data are from at least five unrelated, healthy donors. (B) The geometric mean fluorescence intensity of vedolizumab binding to various subsets of leukocytes. Gating is restricted to the population of the leukocytes that stains positively with vedolizumab. Data are the means from five unrelated, healthy donors with standard deviations indicated by the error bars. GMFI values for each subset were compared to the GMFI of all leukocytes by a two-tailed, homoscedastic Student's T-Test. * denotes $p < 0.05$, ** denotes $p < 0.01$.

Fig. 2. A comparison of the binding of vedolizumab to expression of the α_4 and β_1 chains by human $CD4^+$ T lymphocytes and monocytes. Human peripheral blood was stained with the indicated antibodies and examined by flow cytometry. (A) Blood was stained with vedolizumab, and anti-CD4 and anti-CD45RO antibodies. These plots illustrate the binding of vedolizumab in the total ($CD4^+$), naïve ($CD4^+CD45RO^-$), and memory ($CD4^+CD45RO^+$) $CD4^+$ T cell subsets. The box indicates the level of background signal of the negative population, and the horizontal line denotes the $\alpha_4\beta_7^{hi}$ population. (B) Blood was stained with anti-CD4, -CD45RO, - α_4 , and - β_1 antibodies. These plots illustrate the coexpression of the α_4 and β_1 chains in the total, naïve and

JPET #153973

memory CD4⁺ T cell subsets. (C) Blood was stained with vedolizumab, and anti-CD4, - α_4 , and - β_1 antibodies. Vedolizumab binding was examined in the three $\alpha_4^+\beta_1^+$ CD4⁺ memory T cell populations of the total CD4⁺ T cell plot of panel B: $\alpha_4^{\text{hi}}\beta_1^{\text{lo}}$ (I), $\alpha_4^{\text{hi}}\beta_1^{\text{hi}}$ (II), and $\alpha_4^{\text{lo}}\beta_1^{\text{hi}}$ (III). (D) Blood was stained with vedolizumab and anti-CD14 antibodies. This plot illustrates the binding of vedolizumab to monocytes. (E) Specificity of binding was demonstrated by competition with Act-1. (F) Blood was stained with anti-CD14, - α_4 , and - β_1 antibodies. This plot illustrates coexpression of α_4 and β_1 by monocytes. All data are representative of at least five unrelated, healthy donors.

Fig. 3. The specificity of vedolizumab binding to the $\alpha_4\beta_1$, $\alpha_4\beta_7$, and $\alpha E\beta_7$ integrins. (A) Flow cytometric analysis of vedolizumab binding to cell lines that express exclusively the $\alpha_4\beta_7$ (A and B), $\alpha_4\beta_1$ (C and D), and $\alpha E\beta_7$ (E and F) integrins. The flow cytometry plots represent at least three independent experiments.

Fig. 4. Vedolizumab binds to a subset of Th17 lymphocytes. Flow cytometric analysis illustrates the percentage of human peripheral-blood Th17 lymphocytes that bind vedolizumab and anti- α_4 antibody. Data are the means of at least four unrelated, healthy donors with standard deviations indicated by the error bars. Values for percent of total Th17 population for the positive (+) population were compared to the negative (-) population using a two-tailed, homoscedastic Student's T-Test. * denotes $p < 0.05$, ** denotes $p < 0.01$.

JPET #153973

Fig. 5. Binding of vedolizumab to human peripheral-blood B and memory CD4⁺ T lymphocytes.

(A) Saturation binding curve of vedolizumab-alexa-647 binding to peripheral-blood B lymphocytes (closed circles) and memory CD4⁺ T lymphocytes (open circles). (B) Dose-dependent inhibition curve of vedolizumab-alexa-647 binding to B lymphocytes (closed circles) and memory CD4⁺ lymphocytes (open circles) by unlabelled vedolizumab. Squares are control antibody for B lymphocytes (closed) and memory CD4⁺ T lymphocytes (open). The data represent multiple donors.

Fig. 6. Potency and specificity of vedolizumab antagonism of $\alpha_4\beta_7$ integrin adhesion to MAdCAM-1 and fibronectin, but not to VCAM-1. Effect of vedolizumab (closed circles, A–D, F), a humanized mAb negative control (open triangles, A–B, F), an anti- α_4 mAb (open circles, A–D, F), and isotype control Ig (asterix, A–D, F) on adhesion of $\alpha_4\beta_7$ -expressing RPMI8866 cells to MAdCAM-1 with high (A) and low (B) affinity, to VCAM-1 with high (C and E) and low (D and E) affinity, and to fibronectin with high affinity (F). In panel E: Data are the mean of three independent experiments with standard deviations indicated by the error bars. RFU values for cells incubated with antibody were compared to RFU values for cells not incubated with antibody using a two-tailed, homoscedastic Student's T-Test. * denotes $p < 0.05$, ** denotes $p < 0.01$.

Fig. 7. Vedolizumab antagonism of MAdCAM-1-Fc binding to the $\alpha_4\beta_7^{\text{hi}}$ CD4 memory T lymphocyte population in human peripheral blood *in vitro*. Blood was stained with MAdCAM-1-Fc, with or without vedolizumab, and with anti-CD4 and anti-CD45RO antibodies. MAdCAM-1-

JPET #153973

Fc binding to the CD4 memory T lymphocyte population was analyzed by flow cytometry. Results are reported as the percentage of the total CD4 memory T lymphocyte population that bound MAdCAM-1 versus vedolizumab concentration. Data are the mean of three independent donors.

Fig. 8. Effect of vedolizumab (black circles, A and C), anti- α_4 mAb (white circles, A and C), and isotype control Ig (hatched marks, A and C) on adhesion of cells expressing the $\alpha_4\beta_1$ integrin to VCAM-1 and fibronectin. Effect of mAbs on high- (A and B) and low-affinity (C and D) binding of $\alpha_4\beta_1$ -expressing RAMOS cells to VCAM-1, and effect of mAbs on binding to fibronectin (E). Anti- α_4 mAb, anti- β_1 mAb, mouse IgG at 10 ug/ml, and vedolizumab at 400 ug/ml were used (B, D and E).). In panels B, D and E: Data are the mean of three independent experiments with standard deviations indicated by the error bars. RFU values for cells incubated with antibody were compared to RFU values for cells incubated with mouse IgG using a two-tailed, homoscedastic Student's T-Test. * denotes $p < 0.05$, ** denotes $p < 0.01$.

JPET #153973

TABLE 1

Binding specificity of vedolizumab in normal human tissues.

Tissue	Region	Vedolizumab		Isotype Control	
		20 μ g/ml	2 μ g/ml	20 μ g/ml	2 μ g/ml
Adrenal	Stromal elements	Neg.	Neg.	Neg.	Neg.
Blood cells	Mononuclear cells	1.0	1.0	Neg.	Neg.
	Polymorphonuclear cells	Neg.	Neg.	Neg.	Neg.
	Platelets	Neg.	Neg.	Neg.	Neg.
Blood vessel endothelium	Stromal elements	Neg.	Neg.	Neg.	Neg.
Bone marrow	Stromal elements	Neg.	Neg.	Neg.	Neg.
Brain cerebrum	Stromal elements	Neg.	Neg.	Neg.	Neg.
Brain cerebellum	Stromal elements	Neg.	Neg.	Neg.	Neg.
Breast	Stromal elements	Neg.	Neg.	Neg.	Neg.
Colon	Mononuclear infiltrate	3.0	3.0	Neg.	Neg.
	Stromal elements	Neg.	Neg.	Neg.	Neg.
Cervix	Mononuclear infiltrate	0.5	0.5	Neg.	Neg.
	Stromal elements	Neg.	Neg.	Neg.	Neg.
Esophagus	Mononuclear infiltrate	2.0	1.0	Neg.	Neg.
	Stromal elements	Neg.	Neg.	Neg.	Neg.
Eye	Stromal elements	Neg.	Neg.	Neg.	Neg.
Heart	Stromal elements	Neg.	Neg.	Neg.	Neg.
Kidney	Stromal elements	Neg.	Neg.	Neg.	Neg.
Liver	Stromal elements	Neg.	Neg.	Neg.	Neg.

Downloaded from jpet.aspetjournals.org at ASPET Journals on September 19, 2016

JPET #153973

Lung	Stromal elements	Neg.	Neg.	Neg.	Neg.
Lymph node	Mononuclear infiltrate	1.8	2.2	Neg.	Neg.
	Stromal elements	Neg.	Neg.	Neg.	Neg.
Mammary gland	Stromal elements	Neg.	Neg.	Neg.	Neg.
Ovary	Stromal elements	Neg.	Neg.	Neg.	Neg.
Fallopian tube oviduct	Stromal elements	Neg.	Neg.	Neg.	Neg.
Pancreas	Stromal elements	Neg.	Neg.	Neg.	Neg.
Parathyroid	Stromal elements	Neg.	Neg.	Neg.	Neg.
Peripheral nerve	Stromal elements	Neg.	Neg.	Neg.	Neg.
Pituitary	Stromal elements	Neg.	Neg.	Neg.	Neg.
Placenta	Stromal elements	Neg.	Neg.	Neg.	Neg.
Prostate	Mononuclear infiltrate	2.0	2.0	Neg.	Neg.
	Stromal elements	Neg.	Neg.	Neg.	Neg.
Salivary gland	Mononuclear infiltrate	2.2	1.7	Neg.	Neg.
	Stromal elements	Neg.	Neg.	Neg.	Neg.
Skin	Stromal elements	Neg.	Neg.	Neg.	Neg.
Small intestine	Mononuclear infiltrate	2.7	2.7	Neg.	Neg.
	Stromal elements	Neg.	Neg.	Neg.	Neg.
Spinal cord	Stromal elements	Neg.	Neg.	Neg.	Neg.
Spleen	Mononuclear infiltrate	2.5	2.5	Neg.	Neg.
	Stromal elements	Neg.	Neg.	Neg.	Neg.
Stomach	Mononuclear infiltrate	2.7	2.7	Neg.	Neg.
	Stromal elements	Neg.	Neg.	Neg.	Neg.

JPET #153973

Skeletal Muscle	Stromal elements	Neg.	Neg.	Neg.	Neg.
Testis	Stromal elements	Neg.	Neg.	Neg.	Neg.
Thymus	Mononuclear infiltrate	2.2	2.2	Neg.	Neg.
	Stromal elements	Neg.	Neg.	Neg.	Neg.
Thyroid	Stromal elements	Neg.	Neg.	Neg.	Neg.
Tonsil	Mononuclear infiltrate	2.2	2.2	Neg.	Neg.
	Stromal elements	Neg.	Neg.	Neg.	Neg.
Urinary Bladder	Mononuclear infiltrate	1.7	1.7	Neg.	Neg.
	Stromal elements	Neg.	Neg.	Neg.	Neg.
Uterus	Stromal elements	Neg.	Neg.	Neg.	Neg.

Data are mean values from three samples from three independent donors.

0.0 to 0.3 (equivocal), 0.3 to 1.0 (weak), 1.3 to 2.0 (moderate), 2.3 to 3.0 (strong), 3.3 to 4.0 (intense), Neg. (negative).

Figure 1

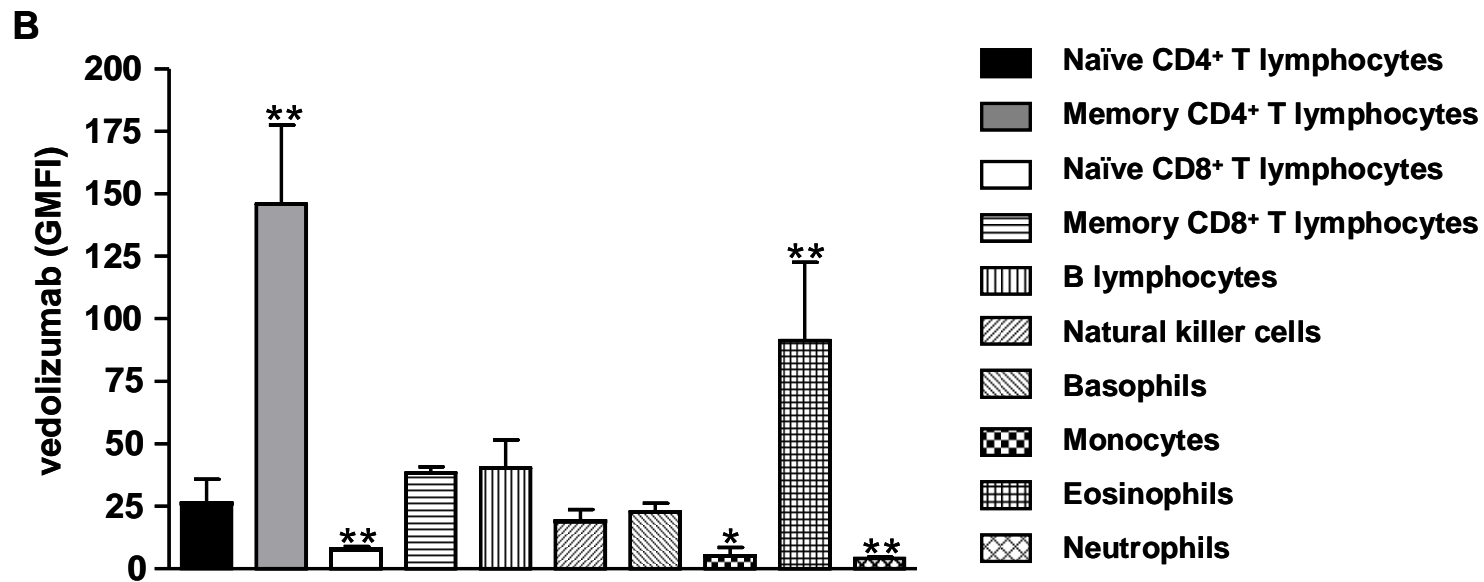
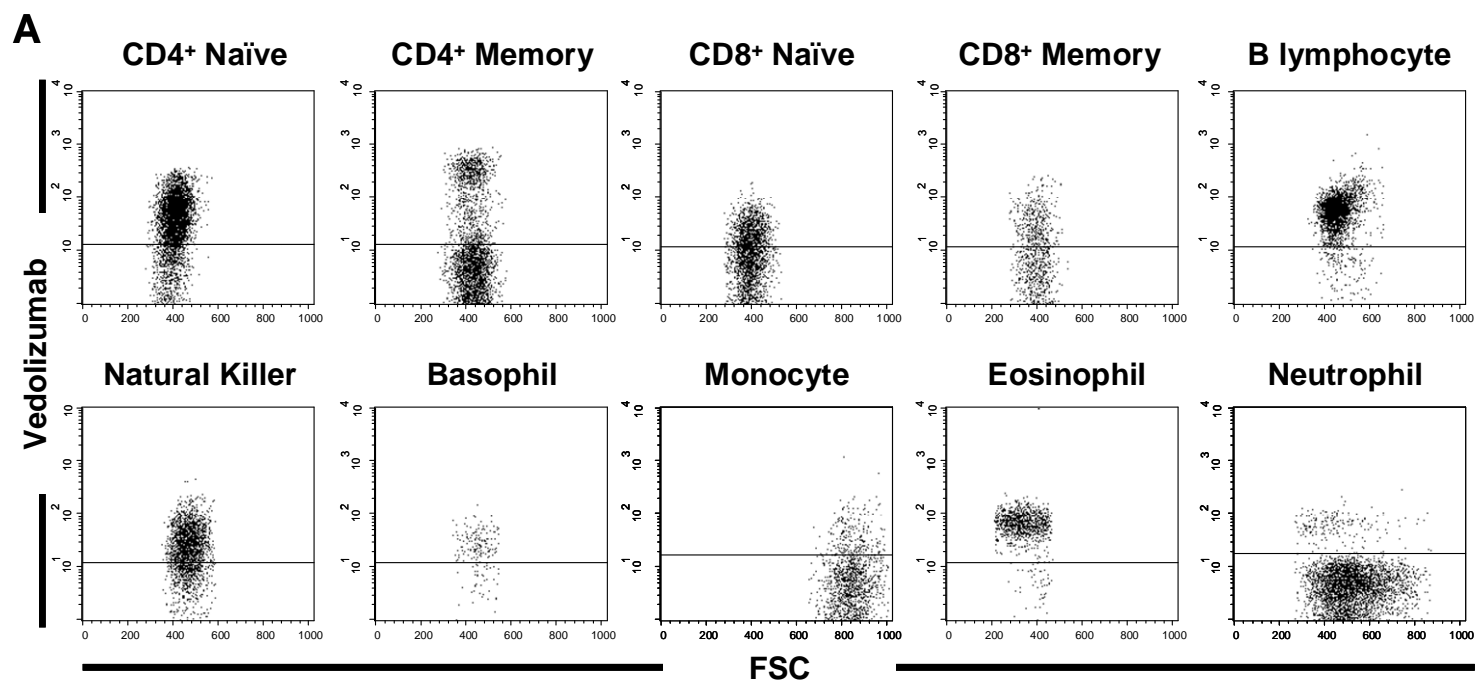


Figure 2

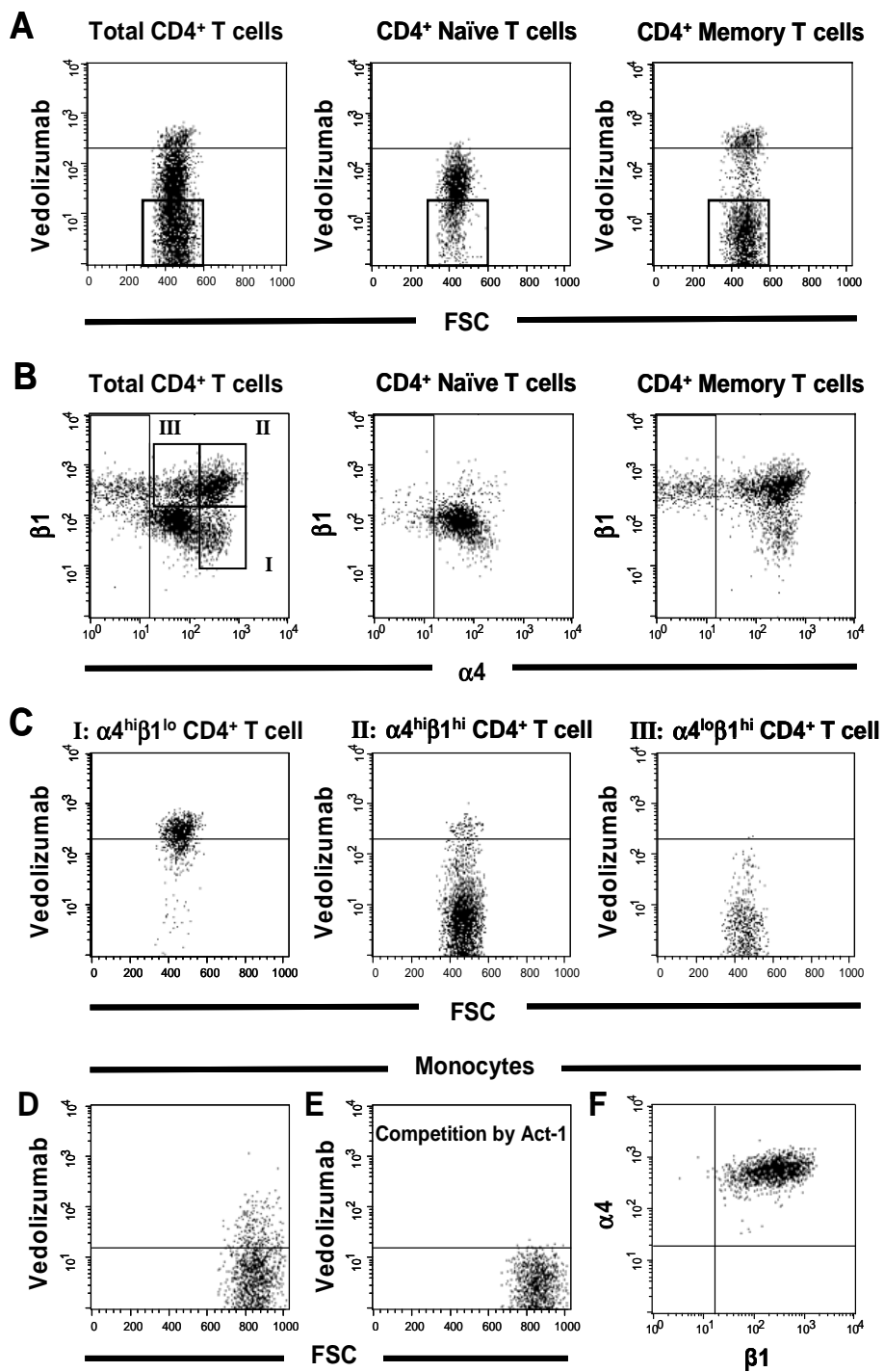


Figure 3

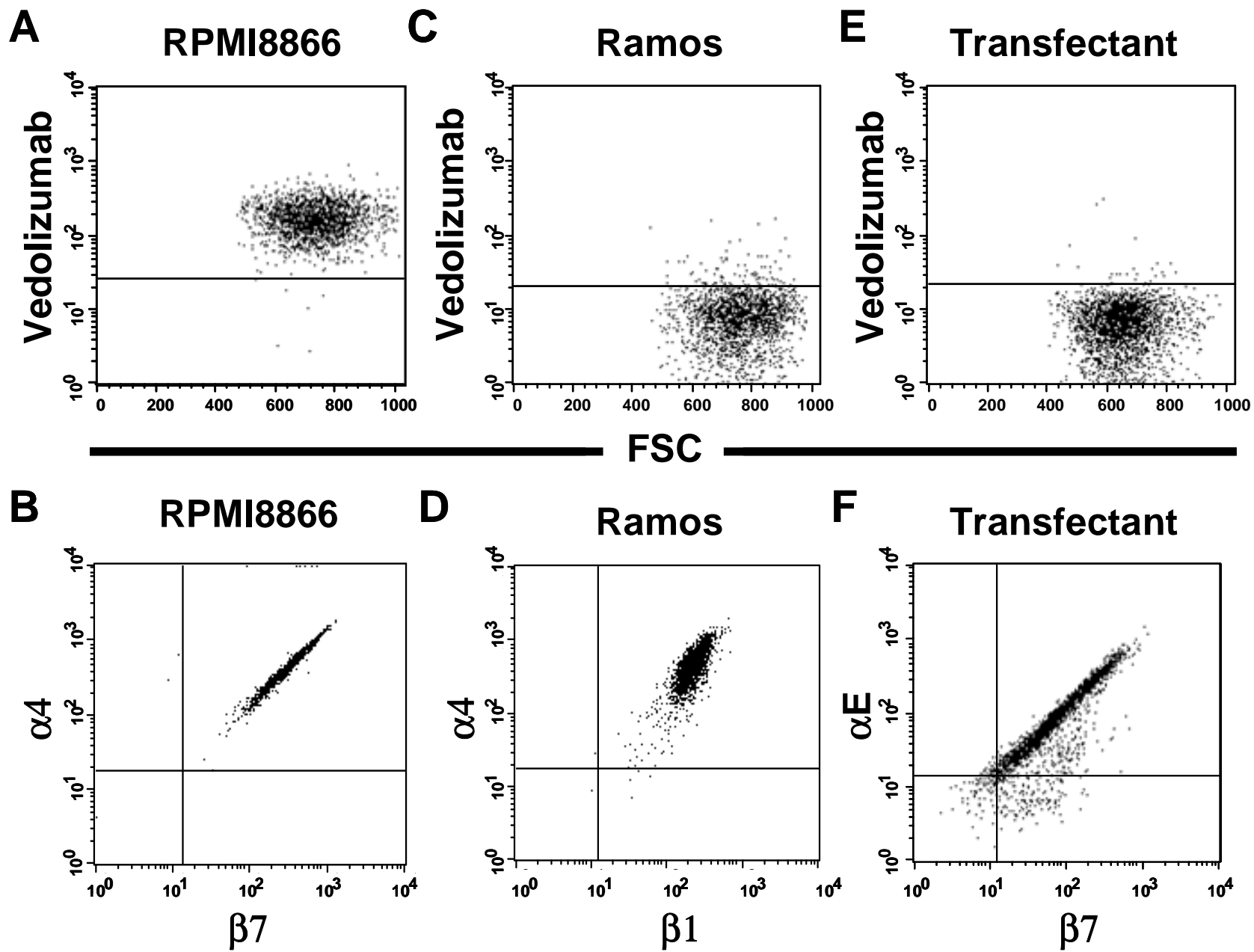


Figure 4

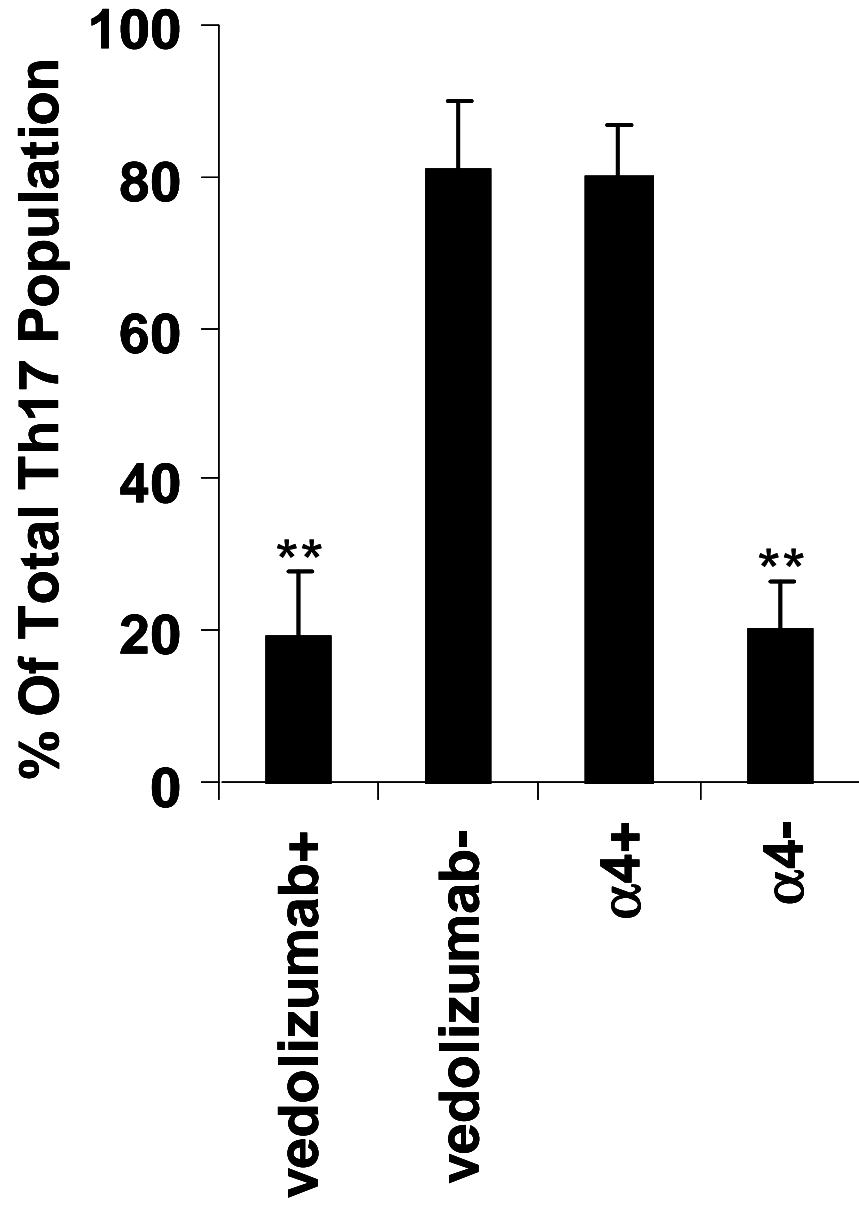


Figure 5

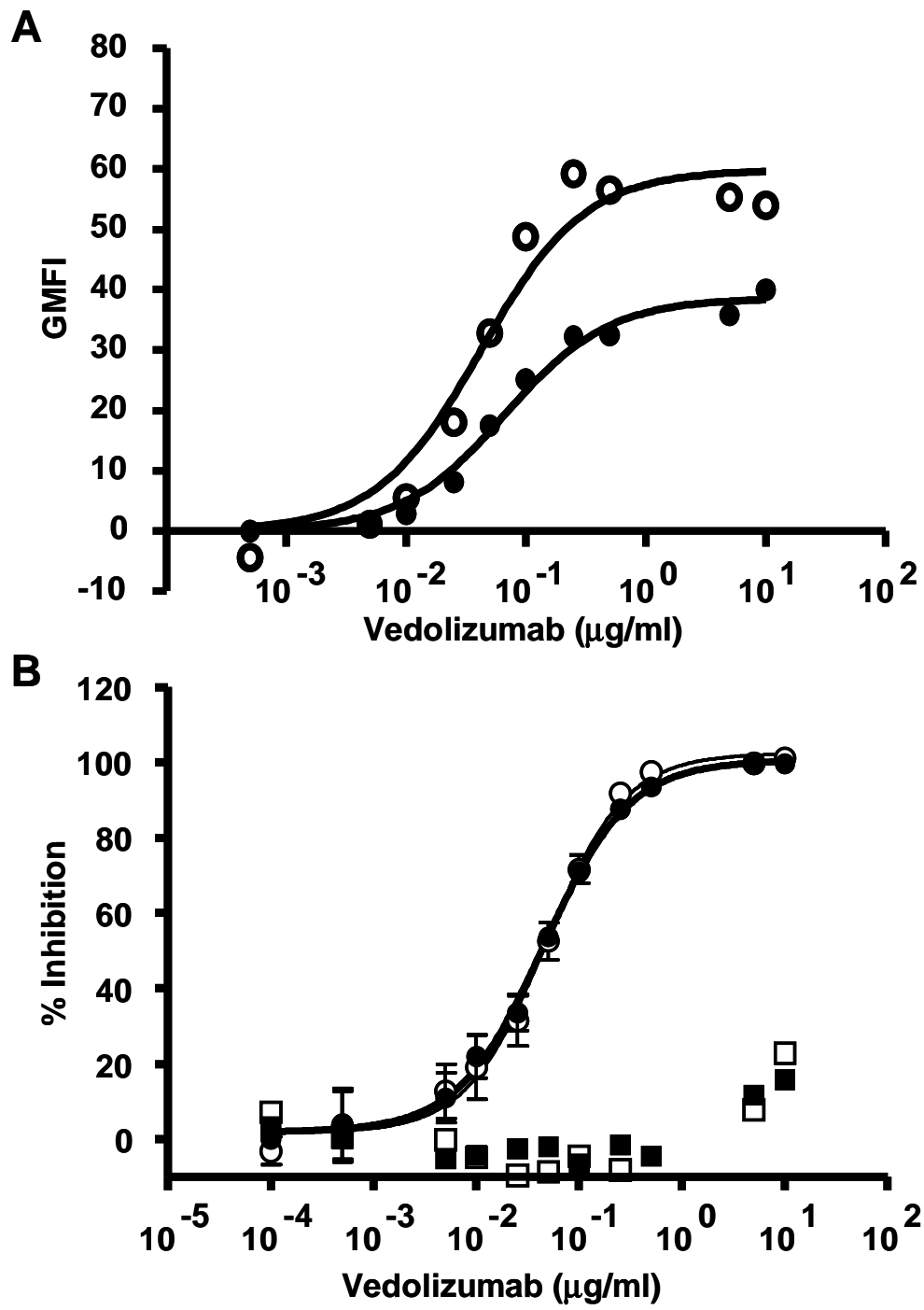


Figure 6

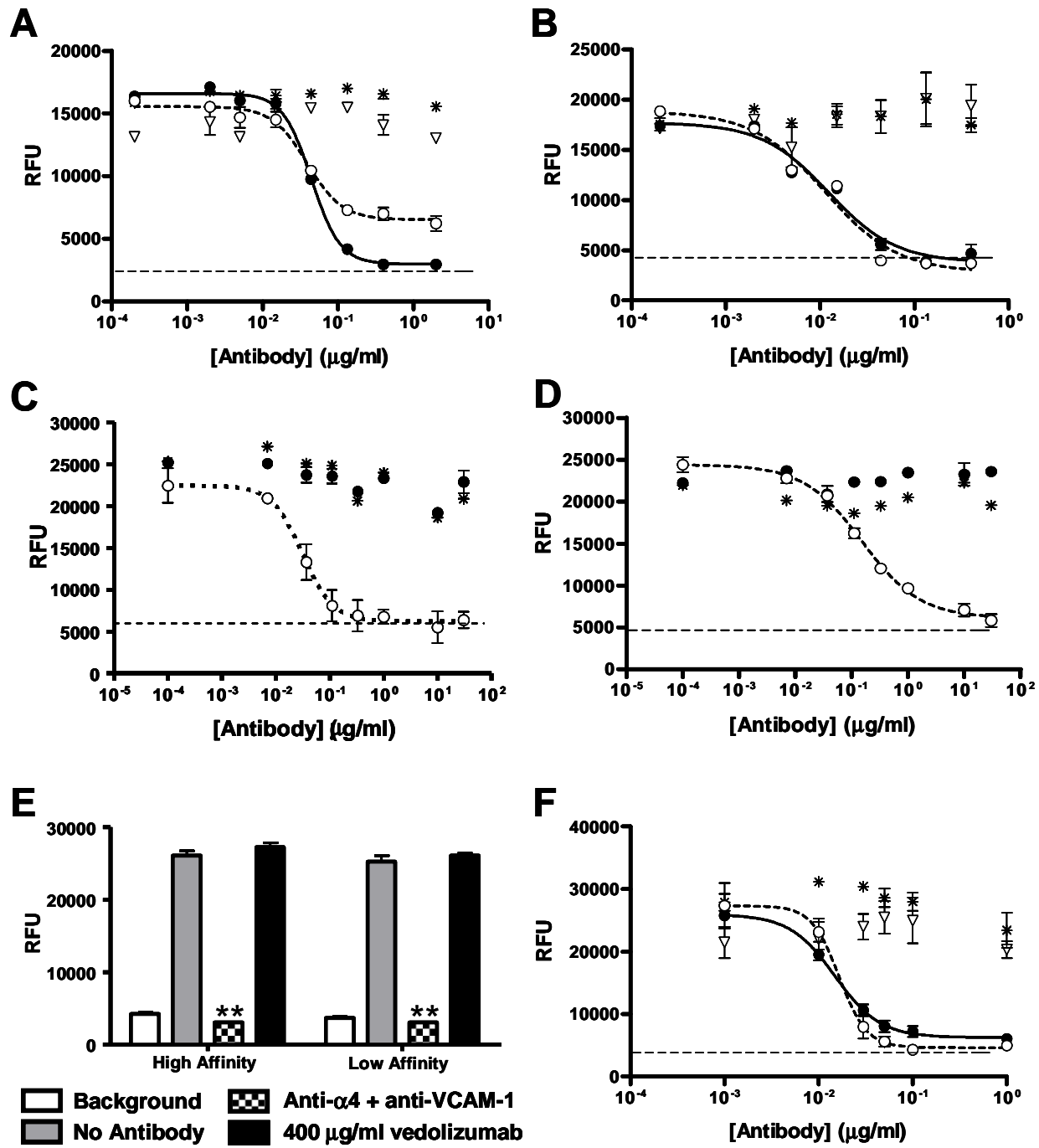


Figure 7

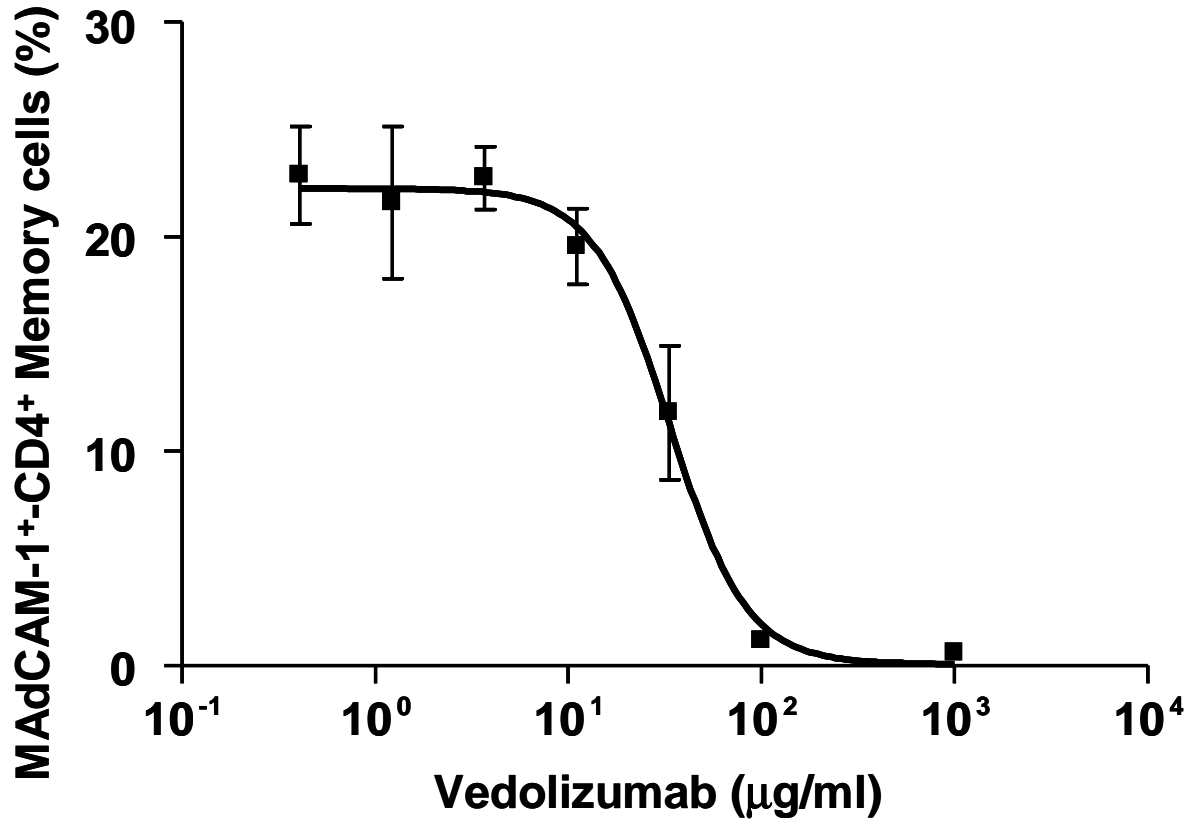


Figure 8

